JES
Journal of Engineering Sciences

Vol 13, Issue 02, FEB /2022

ISSN NO:0377-9254

AN ENHANCED CONTROL PROCEDURE FOR THAT DVR TO ACCOMPLISH BOTH LVRT AND HVRT IN THE DFIG WIND TURBINE

[1]Mr. G.SAI KUMAR, [2]S. RADHA KRISHNA REDDY
[1]PG scholar in Holy Mary Institute of Technology & Science, Bogaram (V), Medchal District, Hyderabad, India in the Dept. of Electrical & Electronics Engineering
[2]Associate Professor in Holy Mary Institute of Technology & Science, Bogaram (V), Medchal District, Hyderabad, India in the Dept. of Electrical & Electronics Engineering.

ABSTRACT: ***For Double Fed Induction Generator (DFIG) wind turbines, a proposal proposes an improved procedure for controlling Dynamic Voltage Restorer (DVR) so that it can carry out both Low Voltage Ride Through (LVRT) and High Voltage Ride through (HVRT) operations simultaneously. DFIG-based wind turbines are extremely sensitive to fluctuations in the grid voltage. Consequently, LVRT and HVRT capabilities are used to increase DFIG performance during grid disturbances. In this study, the Dynamic Voltage Restorer (DVR) has been presented to enhance the capabilities of LVRT and HVRT. MATLAB simulations show that a proposed strategy works as expected.***

Keywords: Double Fed Induction Generator (DFIG), Dynamic Voltage Restorer (DVR), Low Voltage Ride Through (LVRT), and High Voltage Ride Through (HVRT).

I. INTRODUCTION

For the secure and safe energy network, ambitious grid code requirements are needed to handle a rising amount of power generated by decentralized renewable systems, such as wind power. for that example, the grid code includes rules for dealing with faults and steady-state production of active and reactive power. Real grid standards dictate that wind farms should contribute to power system control, such as frequency and voltage control, to behave like conventional power plants. During grid voltage outages, grid codes mandate that wind turbines remain connected and generate a reactive power in the order to support and restore a system's voltage as rapidly as possible.

With variable-speed operation and individually adjustable active and reactive power, a DFIG (double-fed induction generator) is a prominent idea in wind turbines. Because of this, a rotor side of the power electronic converter of DFIGs must be protected from voltage dips that are symmetrical or asymmetrical.

It is common practice to disable an RSC and attach the resistive network known as "crowbar" to a motor circuit in the event of excessive rotor currents or dc-link voltages. As explained in [9], when a crowbar is triggered, a machine draws a huge quantity of reactive power from a power network, which is unacceptable when taking into account actual grid code requirements, resulting in a high short circuit current. in the order to safely navigate grid faults and meet grid codes, different means of protection must be examined. for that fault ride-through of the DFIG, extra hardware such as the series dynamic resistance in a rotor [10] or a stator in the [11] or employing the series line side converter (LSC) architecture as in the [12] have been proposed. [12]

Changing an RSC control to prevent a need for that extra hardware can reduce rotor currents during transient grid voltage fluctuations. Stator voltage feed forward [13], consideration of stator flux linkage [14], or use of observed stator currents as the reference for that a rotor current controller [15] can all be used to safeguard RSCs from damage.

A number of other studies have focused on an enhanced performance when a grid voltage is unsymmetrical [16–19]. A converter in the [20] is protected by the demagnetizing current, but it becomes evident that the crowbar activation cannot be avoided during deep transient dips, and hence continuous reactive power management cannot be assured.

The DFIG system's protection mechanisms can be omitted if the third-party power electronic device is employed to correct a grid voltage problem. [21] introduces the dynamic voltage restorer (DVR) system, which is the voltage source converter connected in the series to a grid to repair defective line voltage. As the result, a DFIG system is made simpler by the use of an external protective device. Drawbacks of DVR include its expense and complexity. in the addition to protecting wind turbines that don't have appropriate fault ride-through behavior, the DVR can be used to protect any distributed load in the micro grid, such as the battery. [22] Compares the power and voltage ratings of several DVR configurations. [23] Describes the DVR operating at medium voltage. In [24] and [25], resonant controllers are used to compensate for those voltages that are not symmetric. In [26], the squirrel cage induction generator's fault ride-through capacity

Journal of Engineering Sciences

Vol 13, Issue 02, FEB /2022

ISSN NO:0377-9254

is provided by the DVR. [27] And [28] provide the DVR for that DFIG wind turbine protection, although only symmetrical voltage dips have been tested, and measurements do not cover transient grid failures and reactive power.

An uninterruptible fault ride-through of voltage dips that meets grid code criteria is examined in this research using the DVR coupled to the DFIG powered by the wind turbine. A DFIG wind turbine can maintain its nominal operation as required by actual grid standards while a DVR compensates for that incorrect line voltage. Measurement results under transient grid voltage dip on the 22 kW laboratory setup are reported here. This paper provides a thorough examination of DFIG behavior and DVR control, which was first described in the [19].

II. MODELING OF CASE STUDY DFIG

Fig. 1 depicts an examined wind turbine system, which comprises of main elements such as a turbine, gear (in most systems), DFIG, and back-to-back voltage source converter with the dc connection (as indicated). here is the DC chopper to reduce a voltage across a dc capacitor, as well as the crowbar. To decrease harmonics, the line filter connects a back-to-back converter to a grid, where an RSC and LSC are connected. A wind turbine is safeguarded by a digital video recorder (DVR). A mechanical element of the turbine's dynamics will be omitted due to a brief duration of voltage disturbances, and a wind-driven mechanical torque will be considered to remain constant.

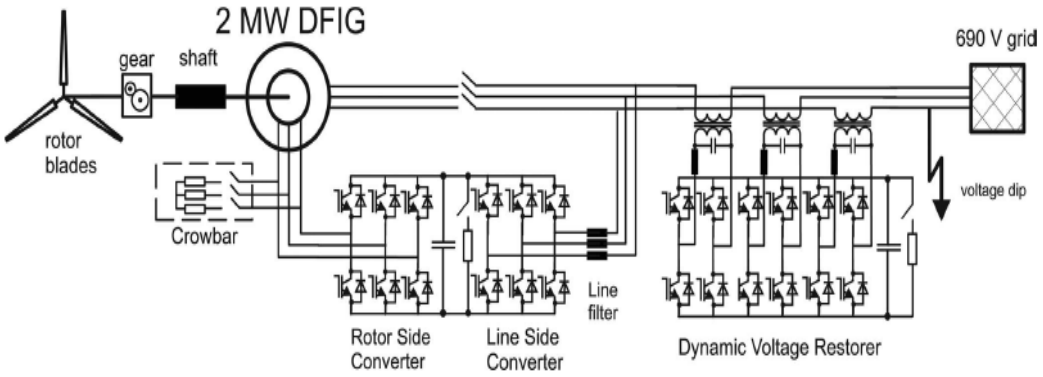

Fig. 1. DVR-enabled DFIG wind turbine system schematics.

a dynamic of rotor voltage

RSC design and operation necessitate an exact understanding of rotor voltage amplitude and frequency. Following [4], we now construct equations for that rotor voltage in the normal operation as well as under symmetrical stator voltage dip. After that, a torque rating of the rotor converter is taken into account, and a process is complete.

The following stator and rotor voltage and flux equations can be derived from a DFIG's per-phase equivalent circuit in the static stator-oriented reference frame:

$$v_s = R_s i_s + \frac{\partial \varphi_s}{\partial t} \quad (1)$$

$$v_r = R_r i_r + \frac{\partial \varphi_r}{\partial t} - j\Omega\varphi_r \quad (2)$$

$$\varphi_r = L_s i_s + L_h i_r \quad (3)$$

$$\varphi_r = L_r i_s + L_h i_r \quad (4)$$

There are three vectors: vamps (flush), verve (voltage), and vici (current). A stator and rotor quantities are denoted by subscripts s and r, respectively. The inductances of stator and rotor are represented by Ls = Ls + Ly and Lr = Lr + Ly, while a mutual inductance is represented by Ly. A stator and rotor resistances are represented by Rs and Rr, while an electrical rotor frequency is represented by.

The rotor flux can be expressed in the terms of rotor current and a stator flux by applying a leakage factor = $\frac{L_h}{L_s}\varphi_s$

$$\varphi_r = \frac{L_h}{L_s}\varphi_s + \sigma L_r i_r \quad (5)$$

A rotor voltage equation can be found by replacing (5) in (2).

$$v_r = \frac{L_h}{L_s}\left(\frac{\partial}{\partial t} - j\Omega\right)\varphi_s + \left(R_r + \sigma L_r\left(\frac{\partial}{\partial t} - j\Omega\right)\right) i_r \quad (6)$$

This is divided into two halves. A stator flux _s, which is normally provided by a constantly revolving vector, causes the first portion of the problem.

$$\varphi_s = \frac{v_s}{j\omega_s} e^{j\omega_s t} \quad (7)$$

The rotor current ire is to blame for that a second portion of (6). in many cases, a rotor resistance Rr and a leakage factor are insignificant, therefore a rotor voltage does not deviate significantly from a stator flux component. A normal rotor voltage amplitude Vr0 can therefore be calculated as

$$v_{r0} \approx v_s \frac{L_h}{L_s}\frac{\omega_r}{\omega_s} = v_s \frac{L_h}{L_s} s \qquad (8)$$

s = 1 (/s) = r/s explains a slip, while r indicates a slip frequency. During full symmetrical stator voltage dips, a rotor voltage has induced a maximum. Stator voltage drops from normal amplitude V1 to faulty amplitude V2 as described under the symmetrical voltage dip.9)

$$v_s = \begin{cases} v_1 e^{j\omega_s t}, \text{for } t < t_0 \\ v_2 e^{j\omega_s t} \text{ for } t \geq t_0 \end{cases} \qquad (9)$$

$$\varphi_s = \begin{cases} \varphi_1 = \frac{v_1}{j\omega_s} e^{j\omega_s t}, < t_0 \\ \varphi_2 = \frac{v_2}{j\omega_s} e^{j\omega_s t} \geq t_0 \end{cases} \qquad (10)$$

As the continuous quantity, a stator flux cannot track a voltage step function. Assuming _ire = 0, due to its low impact on a rotor voltage, a differential equation (11) may be solved for that an evolution of stator flux.

$$\frac{\partial \varphi_s}{\partial t} = v_s - \frac{R_s}{L_s}\varphi_s \qquad (11)$$

The answer is divided into two parts. Following the voltage dip, a SteadyState stator flux is characterized by _s2 while a flux transition from _a too _s2 is described by _s1 (12)

$$\varphi_s = \varphi_{s0} e^{-t\frac{R_s}{L_s}} = \varphi_{s0} e^{\frac{-t}{\tau_s}} \qquad (12)$$

Stator flow prior to and following a voltage dip is defined by (V1 – V2)/jess. A total flow of testator is a sum of two components.

$$\varphi_s(t) = \frac{v_2}{j\omega_s} e^{j\omega_s t} + \frac{v_1 - v_2}{j\omega_s} e^{\frac{-t}{\tau_s}} \qquad (13)$$

Using a rotor voltage equation from (6) and a dynamic stator flux from (13) as input, a rotor voltage dynamic behavior under the symmetrical voltage dip is defined by (15)

$$v_s = \frac{L_h}{L_s}\left(\frac{\partial}{\partial t} - j\Omega\right)\left(\frac{v_2}{j\omega_s} e^{j\omega_s t} + \frac{v_1 - v_2}{j\omega_s} e^{\frac{-t}{\tau_s}}\right) \qquad (14)$$

$$= \frac{L_h}{L_s}\left(s v_2 e^{j\omega_s t} - (1-s)(v_1 - v_2) e^{\frac{-t}{\tau_s}}\right) \qquad (15)$$

It is possible to obtain the following rotor voltage in the frame revolving at rotor frequency:

$$v_r = \frac{L_h}{L_s}\left(s v_2 e^{j\omega_r t} - (1-s)(v_1 - v_2) e^{\frac{-t}{\tau_s}}\right) \qquad (16)$$

The rotor voltage during the symmetrical voltage dip has two components, according to this research. Due to a fact that slip and residual stator voltage are inversely proportional to this initial component's value, it is tiny for that severe voltage dips and low slips. The first part's frequency is a slip frequency (for the slip of 0.2, r = 10Hz). First, a second component of (16) is very high amplitude and rotates at an electrical rotor frequency (= 60Hz) proportional to a (1/s) time constant. Stator time constant s causes a component to degrade exponentially. Rotor voltage will peak at a beginning of fault (t = 0) and during the full dip during symmetrical voltage dips.

(V2 = 0)

$$v_{r,max} \approx \frac{L_h}{L_s}(1-s)v_1 \qquad (17)$$

Notably, in this case, the highest rotor voltage is about 17 millivolts (mV). RSC of DFIGs is rated for that part of stator power because a rotor power is approximately proportional to slip PR sap that is normally between 0.3. Ly/Ls = 1 indicates that a rotor voltage amplitude is likely to be determined by a Ly/Ls ratio.

$$v_r = \frac{sV_s}{N_{sr}} \qquad (18)$$

In this case, Nasr stands for a stator to rotor rotations ratio. in the practical wind-turbine-driven DFIGs, a turns ratio is typically set at half or three-quarters to maximize a dc-link voltage and reduce a converter's current rating. Determine a dc-link voltage by using a formula

$$v_r = \frac{V_{dc}}{2} \qquad (19)$$

where a pulse width modulation (PWM) modulation index m is used. When using carrier-based sinusoidal PWM, a modulation index is 1.0, but when using space vector modulation, it is 1.15. A section's findings add to our knowledge of rotor over-currents during symmetrical grid voltage dips. Only if an RSC can supply an appropriate voltage level can rotor currents be controlled effectively. To avoid harming an insulated gate bipolar transistor (IGBT) or dc capacitor, strong currents pass through diodes when a rotor voltage exceeds converter voltage.

The A. Crowbar Defense

A crowbar is added in the traditional DFIG wind turbines to prevent an RSC from tripping owing to over-currents in a rotor circuit or overvoltage in a dc link when a grid voltage dips, which is the resistive network that is connected to a rotor windings of DFIG. Bypassing a rotor with a series of resistors, a crowbar regulates voltages and directs currents in the safe direction. There are no more RSC pulses when you use it, thus it acts more like the squirrel cage induction machine connected directly to a grid when you do. Reactive power absorption from a stator and a network can further reduce voltage levels, which is not permitted in the actual grid codes [9]. A loss of magnetization produced by an RSC in the nominal state can further reduce a voltage level. A crowbar circuit is also a sign of heightened stress.

Journal of Engineering Sciences

Vol 13, Issue 02, FEB /2022

ISSN NO:0377-9254

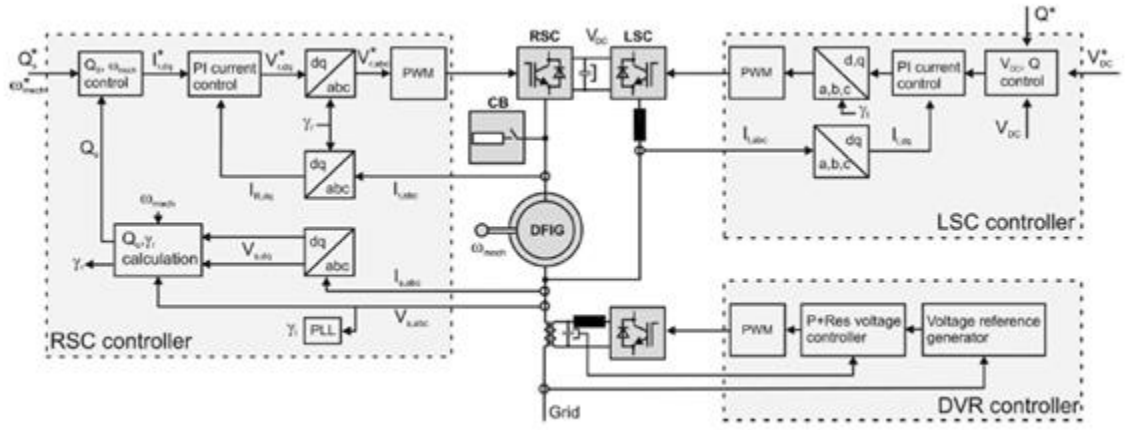

Fig2. DFIG DVR control system

Fig.2. to a system's mechanical components, such as a shaft and gear, as shown in the schematic picture. To learn more about voltage dips and crowbar protection, please refer to [6] and [9]. As the result, crowbar triggering should be avoided from the network and machine mechanical perspective. in any case, simulation results for that crowbar-protected DFIG wind turbines are used to compare a given technique here with a typical DFIG system. in the other words, this is where we design a crowbar resistance. Designing the crowbar resistance is also possible in the [7,9]. A crowbar resistance has the maximum and the minimum set by two limitations. A rotor short-circuits current Irma should be limited by the strong crowbar resistance as the first limitation. Crowbar resistance must be low enough to keep a rotor circuit from overheating, as a second limitation. here will be the significant current flow through anti-parallel diodes when a rotor phase voltage across a crowbar crosses a maximum converter voltage specified in the (18). Simulations employ the crowbar resistance of Crow = 150Rr. With the use of threshold control, it is feasible to inject the demagnetizing current and reduce the duration of the crowbar's operation so that a DFIG may quickly resume normal operation with active and reactive power regulation. the rotor over current triggers the passive crowbar circuit in a laboratory. As soon as safe conditions return, a crowbar can be manually deactivated by a user

III. RSC Control

For decoupled stator control, an RSC is the must-have. in this case, the vector control structure with inner current control loops is used. Figure 2 depicts an overall control system. Control of stator voltage is decomposed into d and q components when stator-voltage oriented (SVO) is used. A stator output active and reactive powers are represented as and without taking into account a stator resistive voltage drop, respectively.

$$P_s = \frac{3L_h}{2L_s} V_{sd} I_{rd} \quad (20)$$

$$Q_s = \frac{3V_{sd}}{2L_s}\left(\frac{V_{sd}}{\omega_s} + L_h I_{rq}\right) \quad (21)$$

As the result, the d and q components of rotor current can be regulated independently of stator active and reactive power. An architecture of outer power control loops is based on (20) and (21).

Controls of LSC

Reactive power is supported by an LSC, which regulates a dc voltage Vdc. Fig. 2 (right) shows the voltage-oriented cascade vector control structure with internal current control loops. A voltage drop across a line inductance LLC can be used to modulate a line current Il, with the following dynamics:

$$v_s = R_l I_l + L_l \frac{\partial I_l}{\partial t} \quad (22)$$

to create a current controller, and to express dc voltage dynamics by

$$C_{dc} \frac{\partial V_{dc}}{\partial t} = I_{dc} - I_{load} \quad (23)$$

Dc capacitance, Idc, and iLoad currents are utilized to create an outer DC voltage control loop, which can be referred to as CDC.

IV. DVR

A. Electrical System

With the line filter, the DVR acts as the voltage source converter (usually LC type). for that sensitive loads or generators, the coupling transformer can be employed as the buffer between a grid and a sensitive load or generator. On a basis of hardware components, switching harmonics, dc-link control, and an ability to inject zero-sequence voltage [31], different transformer-based topologies are compared. According to a DC link connection and power and voltage rating, many system topologies

are examined in the [22]. A depth of voltage fault that needs to be adjusted heavily influences a DVR system rating. Active power needed by a DVR is simply given by when a DC-to-DC voltage fluctuates with the zero-phase angle jump.

$$P_{DVR} = \frac{v_1 - v_2}{v_1} P_{Load} \qquad (24)$$

V1 is a line voltage that is normal, while V2 is one that is malfunctioning. Keep in mind that voltage faults with phase angle jumps, which can result in a higher power rating, require further attention [21].

Voltage controllers employed here are P+RES voltage controllers, which control a voltage across a filter capacitor directly without a need for that internal current controllers. When an inverter voltage reference u* I measured filter capacitor voltage us, and a reference filter capacitor voltage u*c are combined, a controller transfer function is provided by

$$v *_i (s) = v_c(s) + G_P + R_{es}(s).(v *_i (s) - v_c(s)) \qquad (25)$$

where a voltage across a filter capacitor is fed forward. A PRs voltage controller's transfer function is defined as

$$G_P + R_{es}(s) = K_P + K_I \frac{s}{s^2 + \omega_0^2} \qquad (26)$$

It has been discretized and results in a transfer function shown below:

$$G_P + R_{es}(s) = K_P + K_I \frac{zT_s - T_s}{z^2 + (T_s^2 \omega_0^2 - 2) + 1} \qquad (27)$$

A new ant windup feature has also been included. A discrete controller's bode plots and root loci were analyzed to discover control parameters KP and KI. A discrete model of the inverter system includes the delay element in the series with an LC line filter's transfer function.

V. MATLAB CSE STUDY AND SIMULATION RESULTS

Simulations of the 2-MW DFIG wind turbine system and the DVR have been done using MATLAB/Simulink and PLECS to demonstrate the effectiveness of the proposed approach, as shown in Fig. 1. Table I lists the parameters for that simulation. Simulink is used to create a control framework, which can be seen in Figure 2, while PLECS is used to represent all of the power electronic components. To demonstrate the effectiveness of DFIG, we used the two-phase, 37 percent voltage dip lasting 100 milliseconds, both of which were protected by a DVR (see Fig. 3(a) and 4(a)) and displayed in Figures 3 and 4. To a DFIG's response,

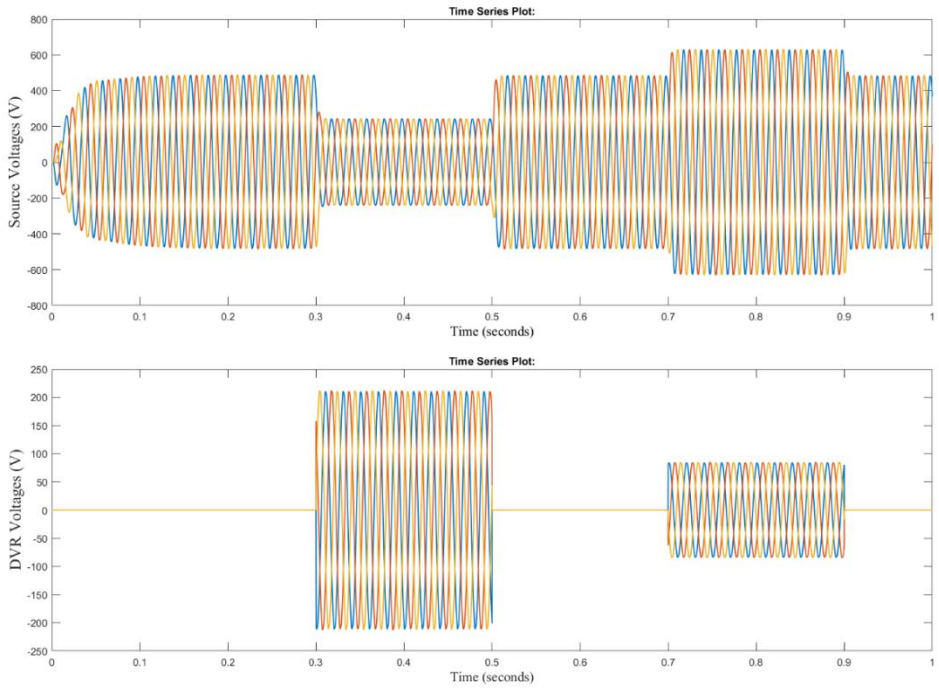

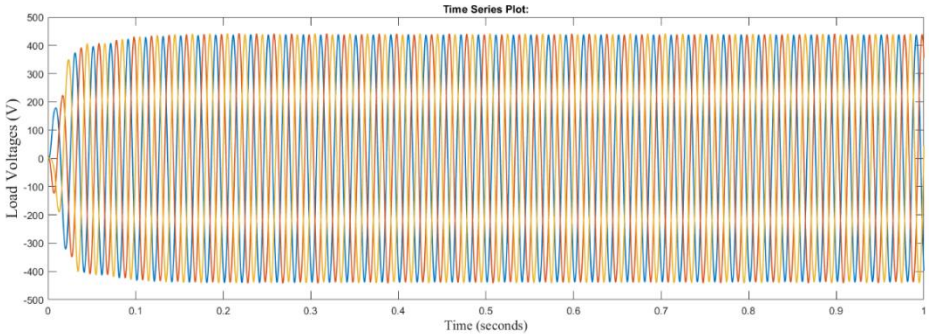

Fig3. Shows a DFIG Voltages, DVR Voltages, and Load Voltages

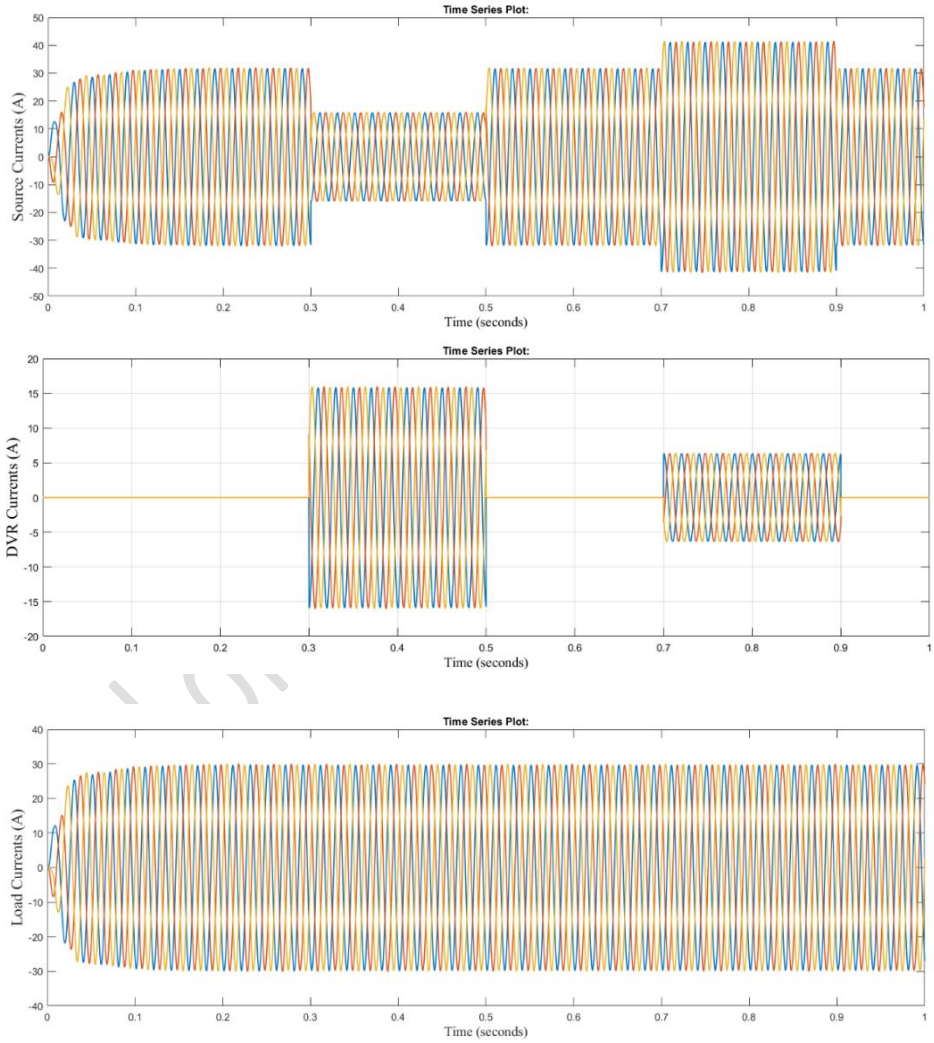

Fig4. Shows DFIG Currents, DVR Currents, and Load Currents.

Journal of Engineering Sciences

Vol 13, Issue 02, FEB /2022

ISSN NO:0377-9254

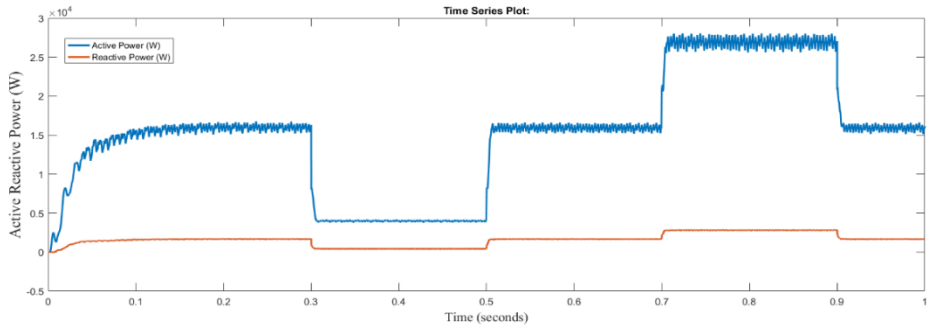

Fig5. Active Reactive power of DFIG.

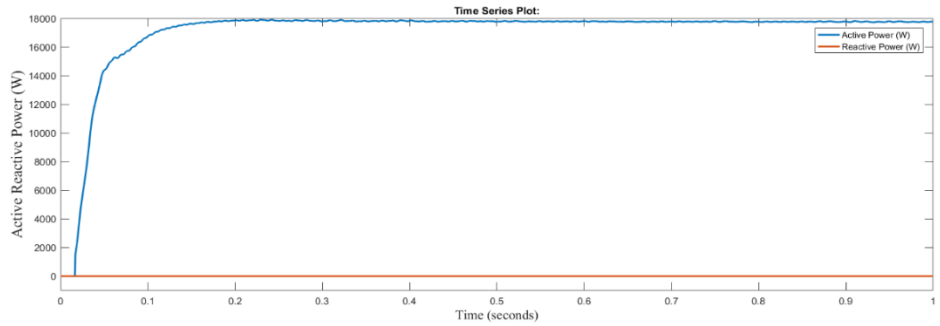

Fig6. Active Reactive power of Load

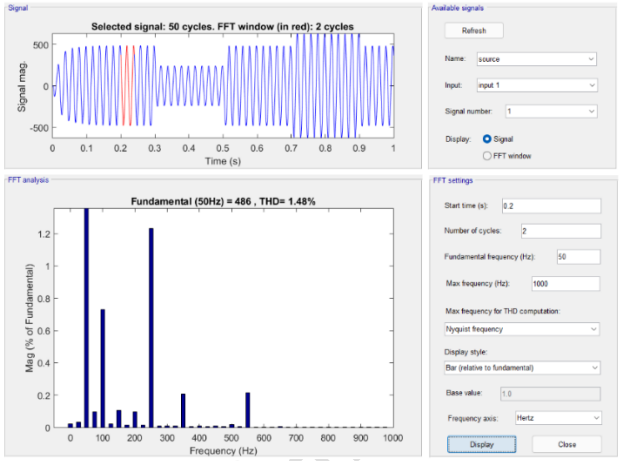

Fig7. THD of DFIG Voltages

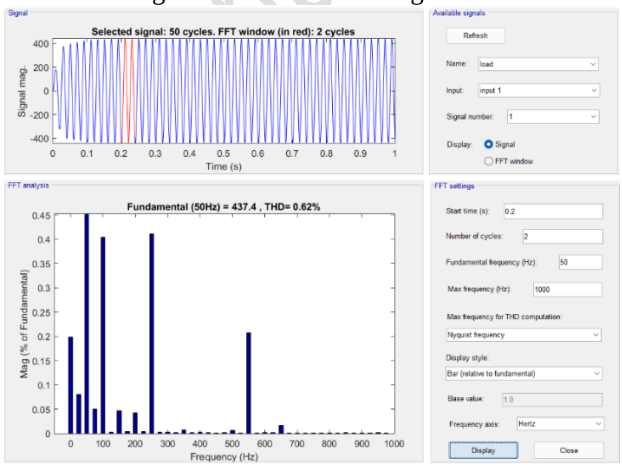

Fig8. THD of Load Voltages

Characterized by high stator currents Because of this, here are substantial currents in the rotor circuit. When rotor currents exceed a maximum level, a crowbar is engaged to protect an RSC from overcurrent's (see Fig. 3(e) and (f)). Once a voltage level has been restored and transients have decreased, a crowbar can be disengaged, but it is not visible here. When a crowbar is active, an RSC can be activated and then deactivated so that a machine excitation is given by a stator. Because grid rules prohibit reactive power control during voltage drops (see Fig. 3(h)), it cannot be done. A rotor is unable to accelerate due to the lack of torque, which may result in the turbine becoming disconnected due to Over speed. A DVR is not turned on in the simulations, as shown in Figure 3. When a wind turbine system is protected by a DVR, a voltage drop can be virtually completely corrected, as shown in the Fig. 4 [see Fig. 4(c)]. As the result of DFIG's response, lower stator and rotor over-currents are created, which implies that a crowbar does not need to be actuated. Despite a fact that a voltage dip is fully adjusted, there is little distortion in the stator currents (dc components) and hence disturbed rotor currents. An RSC, on the other hand, is still functioning and can independently manage a stator's active and reactive power. During the grid fault, reactive power production (Qs=0.5Mvar) is thus maintained at the same rate as needed by grid codes. Remember that DVR and DFIG must communicate. A DVR power necessary to compensate for that voltage drop is depicted in

Figure 4(I). As the result of grid failure, a DVR must consume active and reactive electricity that could not be fed into a broken grid.

CONCLUSION

The use of the DVR coupled to the wind-turbine-powered DFIG to allow uninterruptible fault ride-through of grid voltage faults is being researched. A DVR can compensate for that defective line voltage, allowing a DFIG wind turbine to operate normally and meet any grid code requirements without a need for that extra protective techniques. A DVR can be used to safeguard existing wind turbines that do not have adequate fault ride-through behavior, as well as to protect any distributed load in the microgrid. A simulation results for that the 2 MW wind turbine under an asymmetrical two-phase grid fault demonstrate the effectiveness of the suggested technique when compared to a DFIG's low-voltage ride through employing the crowbar where continuous reactive power production is problematic. To validate results, measurement results during transient grid voltage dips on the 22 kW laboratory setup are reported.

REFERENCES

[1] M. Stile and S. Papathanassiou, "A review of grid code technical requirements for that wind farms," Renewable Power Generat., IET, vol. 3, no. 3, pp. 308–332, Sep. 2009.
[2] R. Pena, J. Clare, and G. Asher, "Doubly fed induction generator using back-to-back pwm converters and its application to variable-speed windenergy generation," Electr. Power Appl., IEE Proc., vol. 143, no. 3, pp. 231–241, May 1996.
[3] S.Muller,M.Deicke, andR.DeDoncker, "Doubly fed induction generator systems for that wind turbines," IEEE Ind. Appl.Mag., vol. 8, no. 3, pp. 26–33, May/Jun. 2002.
[4] J. Lopez, E. Gubia, P. Sanchis, X. Roboam, and L. Marroyo, "Wind turbines based on doubly fed induction generator under asymmetrical voltage dips," IEEE Trans. Energy Convers., vol. 23, no. 1, pp. 321–330, Mar. 2008.
[5] M. Mohseni, S. Islam, and M. Masoum, "Impacts of symmetrical and asymmetrical voltage sags on dfig-based wind turbines considering phaseangle jump, voltage recovery, and sag parameters," IEEE Trans. Power Electron., to be published.
[6] S. Seman, J. Niiranen, and A. Arkkio, "Ride-through analysis of doubly fed induction wind-power generator under unsymmetrical network disturbance," IEEE Trans. Power Syst., vol. 21, no. 4, pp. 1782–1789, Nov. 2006.
[7] W. Zhang, P. Zhou, and Y. He, "Analysis of by-pass resistance of an active crowbar for that doubly-fed induction generator based wind turbines under grid faults," in the Proc. Int. Conf. Electr. Mach. Syst. (ICEMS), Oct., 2008, pp. 2316–2321.
[8] G. Pannell, D. Atkinson, and B. Zahawi, "Minimum-threshold crowbar for that the fault-ride-through grid-code-compliant dfig wind turbine," IEEE Trans. Energy Convers., vol. 25, no. 3, pp. 750–759, Sep. 2010.
[9] J. Morren and S. de Haan, "Short-circuit current of wind turbines with doubly fed induction generator," IEEE Trans. Energy Convers., vol. 22, no. 1, pp. 174–180, Mar. 2007.
[10] J. Yang, J. Fletcher, and J. O'Reilly, "A series-dynamic-resistor-based converter protection scheme for that doubly-fed induction generator during various fault conditions," IEEE Trans. Energy Convers., vol. 25, no. 2, pp. 422–432, Jun. 2010.
[11] A. Causebrook, D. Atkinson, and A. Jack, "Fault ride-through of large wind farms using series dynamic braking resistors (march 2007)," IEEE Trans. Power Syst., vol. 22, no. 3, pp. 966–975, Aug. 2007.
[12] P. Flannery and G. Venkataramanan, "Unbalanced voltage sag ridethrough of the doubly fed induction generator wind turbine with series grid-side converter," IEEE Trans. Ind. Appl., vol. 45, no. 5, pp. 1879– 1887, Sep./Oct. 2009.
[13] J. Liang,W. Qiao, and R. Harley, "Direct transient control of wind turbine driven dfig for that low voltage ride-through," in the Proc. IEEE Power Electron. Mach. Wind Appl. (PEMWA), Jun. 2009, pp. 1–7.
[14] D. Xiang, L. Ran, P. Tavner, and S. Yang, "Control of the doubly fed induction generator in the wind turbine during grid fault ride-through," IEEE Trans. Energy Convers., vol. 21, no. 3, pp. 652–662, Sep. 2006.
[15] F. Lima, A. Luna, P. Rodriguez, E. Watanabe, and F. Blaabjerg, "Rotor voltage dynamics in the a doubly fed induction generator during grid faults," IEEE Trans. Power Electron., vol. 25, no. 1, pp. 118–130, Jan. 2010.
[16] P. Zhou,Y. He, and D. Sun, "Improved direct power control of the dfig-based wind turbine during network unbalance," IEEE Trans. Power Electron., vol. 24, no. 11, pp. 2465–2474, Nov. 2009.
[17] G. Abad, M. Rodriguez, G. Iwanski, and J. Poza, "Direct power control of doubly-fed-induction-generator-based wind turbines under unbalanced grid voltage," IEEE Trans. Power Electron., vol. 25, no. 2, pp. 442–452, Feb. 2010.
[18] L. Xu, "Coordinated control of dfig's rotor and grid side converters during network unbalance," IEEE Trans. Power Electron., vol. 23, no. 3, pp. 1041–1049, May 2008.

[19] D. Santos-Martin, J. Rodriguez-Amenedo, and S. Arnaltes, "Providing ride-through capability to the doubly fed induction generator under unbalanced voltage dips," IEEE Trans. Power Electron., vol. 24, no. 7, pp. 1747–1757, Jul. 2009.
[20] J. Lopez, E. Gubia, E. Olea, J. Ruiz, and L. Marroyo, "Ride through of wind turbines with doubly fed induction generator under symmetrical voltage dips," IEEE Trans. Ind. Electron., vol. 56, no. 10, pp. 4246–4254, Oct. 2009.
[21] M. H. J. Bollen, Understanding Power Quality Problems Voltage Sags and Interruptions. New York: Wiley, 2000.
[22] J. Nielsen and F. Blaabjerg, "A detailed comparison of system topologies for that dynamic voltage restorers," IEEE Trans. Ind. Appl., vol. 41, no. 5, pp. 1272–1280, Sep./Oct. 2005.
[23] C. Meyer, R. De Doncker, Y. W. Li, and F. Blaabjerg, "Optimized control strategy for that the medium-voltage dvr;theoretical investigations and experimental results," IEEE Trans. Power Electron., vol. 23, no. 6, pp. 2746– 2754, Nov. 2008.
[24] Y. W. Li, F. Blaabjerg, D. Vilathgamuwa, and P. C. Loh, "Design and comparison of high-performance stationary-frame controllers for that dvr implementation," IEEE Trans. Power Electron., vol. 22, no. 2, pp. 602–612, Mar. 2007.
[25] F. Marafao, D. Colon, J. Jardini, W. Komatsu, L. Matakas, M. Galassi, S. Ahn, E. Bormio, J. Camargo, T. Monteiro, and M. Oliveira, "Multiloop controller and reference generator for that the dynamic voltage restorer implementation," in the Proc. 13th Int. Conf. Harmon. Quality Power (ICHQP), Oct. 2008, pp. 1–6.

AUTHOR'S BIOGRAPHY

G. SAI KUMAR received the B.Tech. Degree in EEE from JNIT ENGG College, Ibrahim Patnam, Ranga Reddy(Dt), Andhra Pradesh, India, in the year 2015 from JNTUH University. Pursuing M. Tech in Electrical Power Systems in Holy Mary Institute of Technology & Sciences, Bogaram, R.R. District, Hyderabad, and Telangana, India. His favourite topics include Renewable energy resources, DFIG, industrial drives, power systems, power systems, control systems, HVDC and Reactive power compensation techniques.

S.RADHA KRISHNA REDDY received the **B.Tech**. Degree in **EEE** from MITS ENGG College, Madanapalle, Chittor(Dt), Andhra Pradesh, India, from JNTU University and **M. Tech** in **Power Electronics** from S.K. University in the year 2007. He has teaching experience of **16** years & currently working as Associate Professor in Holy Mary Institute of Technology &Science, Bogaram(V),Medchal Dist, Hyderabad ,India in the Dept. of Electrical & Electronics Engg & **Pursuing Ph.D.** in **JNTUH, Hyderabad**, **India**. He published **57** research papers in reputed National & International Journals and **23** papers in International and National conferences attended **10** workshops. His Interest areas are Neural Networks, Power Electronics & Drives, Distributed Generation (DG) & FACTS, etc.